Portulaca oleracea leaf extract as a green corrosion inhibitor for mild steel in 1 M HCl

M.T. Hayajneh,* M.A. Almomani and W.M. AlSharman

Industrial Engineering Department, Faculty of Engineering, Jordan University of Science and Technology, P.O. Box 3030, Irbid, 22110, Jordan
**E-mail: hayajneh@just.edu.jo*

Abstract

Portulaca oleracea leaf extract (POLE) was tested for corrosion inhibition on mild steel in 1 M HCl solution using the potentiodynamic polarization (PDP) and weight loss tests with different concentrations at room temperature. The results suggest that POLE is an excellent corrosion inhibitor and the inhibition efficiency is concentration and time-dependent. The inhibition efficiency increases with increasing POLE concentration and immersion time. The maximum inhibitory efficiency of 93.84% was observed at a concentration of 4 g/L at room temperature. As can be seen from the PDP test, the POLE behaves as a mixed inhibitor and the anodic effect is predominant. The results show that POLE inhibited the corrosion process through the physical adsorption mechanism according to the Langmuir adsorption isotherm model. The Fourier Transform Infrared Spectrometer (FTIR) confirmed the presence of several functional groups with heteroatoms, while the adsorption phenomenon was verified using the UV-visible spectroscopy technique. The results ensure that POLE can form an effective barrier and control corrosion. The obtained results of various tests proved that POLE is an effective green inhibitor for the corrosion of mild steel in an acidic solution.

Received: February 19, 2024. Published: May 23, 2024 doi: 10.17675/2305-6894-2024-13-2-18

Keywords: *corrosion, green inhibitor, mild steel, polarization, weight loss, Portulaca oleracea.*

Notation

i_{corr}^{0}: Corrosion current densities in the absence of the inhibitor in 1 M HCl;
i_{corr}: corrosion current densities in the presence of the inhibitor in 1 M HCl;
η%: inhibitions efficiency based on corrosion current density;
E_{corr}: corrosion potential;
β_a: Tafel anodic slope;
β_c: Tafel cathodic slope;
Δw: average weight loss;
w_0: weight loss of the substrates in the absence of the inhibitor in 1 M HCl;
w_i: weight loss of the substrates in the presence of the inhibitor in 1 M HCl;
C_R: corrosion rate;

ρ: density of the mild steel;
A: area of the mild steel sample;
t: the period of immersion in hours;
C_{R_0} : corrosion rate of the substrates in the absence of the inhibitor in 1 M HCl;
C_R: corrosion rate of the substrates in the presence of the inhibitor in 1 M HCl;
%*IE*: inhibition efficiency based on weight loss;
θ: degree of the surface coverage;
c: inhibitor concentrations;
f: corrosion inhibitor interaction parameter;
k_{ads}: the adsorption equilibrium constant;
R^2: correlations coefficients;
ΔG^0_{ads} : the standard adsorption free energy;
R: gas constant 8.314 J/mol;
T: absolute temperature 298 K;
$1 \cdot 10^6$: concentration of the water molecules in mg/l.

1. Introduction

Corrosion occurs when a metal reacts with a chemical in its environment, causing the metal surfaces to change from unstable to stable through an electrochemical process [1]. Corrosion inhibition plays a crucial role in various industries and applications where metals are used. Corrosion, the gradual degradation of materials, especially metals, due to chemical reactions with the environment, can lead to significant economic losses, safety hazards, and environmental damage. Corrosion inhibition finds applications across a wide range of industries and sectors, each with its unique requirements and challenges such as the oil and gas industry, aerospace and aviation, automotive industry, marine and shipbuilding, and chemical processing industry [2]. The most widely used form of steel is mild steel, which is also referred to as low-carbon steel due to its relatively low carbon content, typically ranging from 0.08% to 0.28% [3]. Mild steel finds application in various manufacturing and construction sectors, including chemical reactors, storage tanks, heat exchangers, and transporting pipelines [4]. Metal alloys, particularly mild steel, are now extensively utilized in numerous industrial applications due to their affordability compared to other alloys, ready availability, high ductility, and good mechanical resistance [5].

Mild steel has been observed to corrode rapidly and with little corrosion resistance after a short period. To remove scales, oxide, and surface contaminants, acid solutions are used in a variety of industrial processes such as acid cleaning, descaling, and pickling. Hydrochloric (HCl), sulfuric (H_2SO_4), phosphoric (H_3PO), and nitric (HNO_3) acids are commonly utilized cleaning agents. The most frequently used acids among these are HCl and H_2SO_4 because they are readily available, efficient, and manageable [6]. Although HCl is more expensive than H_2SO_4, it is usually used because of its less cleaning time, better surface quality, and the cleaning process at low temperatures [7]. Unfortunately, when mild

steel is exposed to these acids, its corrosion rate speeds up, causing material damage and economic losses [8].

Therefore corrosion inhibition plays a critical role in various industries and applications where metals are exposed to corrosive environments such as the oil and gas industry, aerospace and aviation, automotive industry, and marine and offshore structures. So, corrosion inhibition is essential across various industries and applications to mitigate the detrimental effects of corrosion, ensure operational safety, prolong the service life of assets, and reduce maintenance costs. By employing suitable corrosion inhibition strategies and technologies, industries can enhance productivity, protect valuable assets, and promote sustainable practices.

Many protection techniques can be used to control mild steel corrosion, including coating, cathodic protection, anodic protection, and corrosion inhibitors. The corrosion inhibitors are the simplest and most effective method of controlling mild steel corrosion. They are also the most cost-effective method. However, the corrosion inhibitors are usually added in small amounts to acidic solutions to lower the corrosion rate of the metals [7, 9].

Generally, inhibitors are classified as organic or inorganic. Organic inhibitors contain a large number of active compounds that contain heteroatoms (*e.g.*, (O), (N), (S), (P), and/or (Q) bonds in their molecular structure [10–13]. These heteroatoms can be absorbed through the metal surface and block the active sites, forming a thin film, thus decreasing the corrosion rate [14]. It should be mentioned that most organic and synthetic inhibitors are toxic, expensive, and dangerous to humans and the environment [6].

Corrosion protection research in recent years has focused on using efficient, non-toxic corrosion inhibitors, often called green organic inhibitors, which are extracted in extract form from natural products. These inhibitors can be extracted from seeds, leaves, roots, bark, fruits, and medicinal plants [15]. Green organic corrosion inhibitors are also used for different metals such as aluminum, copper, and mild steel. Green organic corrosion inhibitors contain chemical compounds like alkaloids and flavonoids. They also contain amino acids and proteins. They are renewable, eco-friendly, biodegradable, and cost-effective. The active compounds are easily extracted with simple methods. They are environmentally friendly and compatible with humans and the environment [16].

Many researchers have studied the use of plant extracts as corrosion inhibitors for mild steel in acidic media. Hayajneh *et al.* [17] investigated the potential of Jordanian green natural agro-wastes as green organic corrosion inhibitors for mild steel corrosion in HCl solutions. The authors examine ten green inhibitors, identifying the most effective ones as green zucchini leaf extract (CPLE), oak leaf extract (QLE), and okra leaf extract (AELE). Through corrosion tests, including potentiodynamic polarization and weight loss, the researchers highlight these agro-wastes' considerable corrosion inhibition capabilities. The maximum efficiency obtained for CPLE was 95.43% at 500 ppm, 94.42% at 800 ppm for QLE, and 95.07% for AELE at 500 ppm. Almomani *et al.* [18] investigated the corrosion inhibition capabilities of *Ceratonia siliqua* L. pulp extract on mild steel exposed to a 1 M solution of HCl. Through potentiodynamic polarization and weight loss tests at room

temperature, the results indicate that the pulp extract acts as an effective corrosion inhibitor. The inhibition efficiency is influenced by both concentration and time, with higher concentrations and longer immersion times increasing efficiency. At a concentration of 800 ppm, the extract achieves a maximum observed inhibition efficiency of 92.32%. Dehghani and Ramezanzadeh [19] investigated the effect of Rosemary leaf extract as a corrosion inhibitor to protect mild steel in 1 M HCl. The result revealed that the extract of the leaves reduces the mild steel corrosion rate with a high inhibition efficiency of 92% at a concentration of 800 ppm. The thermodynamic data showed that the adsorption process was dominated by chemisorption and obeys the Langmuir adsorption isotherm [20]. The inhibitory behavior of an aqueous extract of eucalyptus leaves was studied by Dehghani *et al.* [1]. The results of their study showed that an 88% inhibition efficiency was obtained using 800 ppm ELE after 2.5 hours of exposure. The thermodynamic parameters indicate that the inhibitor molecules are adsorbed on the surface of the mild steel via physical and chemical interaction. Electrochemical studies revealed that ELE reduces the anodic and cathodic reaction rates, with slight cathodic prevalence. Guruprasad and Sachin [21] reported *Amorphophallus paeoniifolius* leaves (APL) extract for protection of mild steel in 1 M HCl using electrochemical tests. Their experimental studies indicated that 92.49% protection ability could be obtained at a 10% v/v concentration. Keramatinia *et al.* [22] reported an experimental and theoretical study of Nettle leaf extract for mild steel protection in 1 M HCl solution. It was found that 93.90% inhibition efficiency could be achieved at 600 ppm after 1.5 hours of immersion. After a longer exposure time, the inhibition efficiency remains above 80%.

As summarized above, numerous extracts have been utilized as corrosion inhibitors. A majority of these extracts are sourced locally, making the enrichment of local and natural compounds highly advantageous to the industry. One such compound is purslane (*Portulaca oleracea* L.), a warm, annual herbaceous plant belonging to the Portulacaceae family. This plant is known by various names across different countries, such as purslane in Australia and the USA, purslane in Egypt, pigweed in England, pourpier in France, and Ma-chi-Xian in China. Thriving in tropical and subtropical regions worldwide, purslane is commonly consumed as a Potherb and added to soups and salads in Mediterranean and tropical Asian countries [23]. Portulaca oleracea has a long history as a folk medicine in numerous countries, exhibiting various medicinal properties including febrifuge, antiseptic, and anthelmintic effects. Furthermore, it possesses a broad spectrum of pharmacological benefits, such as antibacterial, antiulcer, anti-inflammatory, antioxidant, and wound-healing properties. The World Health Organization recognizes *Portulaca oleracea* as one of the most widely used medicinal plants, often referred to as the “world panacea” [24]. Rich in phytochemical components, this plant offers a plethora of substances such as flavonoids, alkaloids, α-linolenic acid, linoleic acid, omega-3 fatty acids, terpenoids, sugars, vitamins, sterols, proteins, and minerals [25].

The significance of corrosion inhibition research lies in addressing current gaps in knowledge and technology to improve corrosion protection across industries. So, this study

aims to explore the potential of *Portulaca Oleracea* L. leaf extract (POLE) as a natural corrosion inhibitor for safeguarding mild steel in a highly corrosive 1 M HCl solution. Corrosion inhibition was investigated using Potentiodynamic Polarization (PDP) and weight loss techniques. To enhance the assessment of the phytochemical composition of POLE, Fourier Transform Infrared (FTIR) spectra and UV-visible spectroscopy of the extract were employed.

2. Experimental Work

2.1. Preparation of the material

The sample used in this investigation was mild steel. The mild steel samples that the supplier provided, with the following weight percentage and chemical composition (C: 0.08–0.12, Si: 0.3, Mn: 0.25–0.5, S: 0.04, P: 0.03, Cr: 0.1, Cu: 0.3, As: 0.08, and Fe is balanced), were used for the tests. To cut the test samples, 0.1 cm thick mild steel sheet with carbon content (0.08–0.12 wt%) was used. Two sizes of square samples were cut from sheet metal. Samples measuring (6×6) cm^2 were used for potentiodynamic tests and (3×3) cm^2 were used for weight loss tests. The surface of the sample was covered with an adhesive except for a circular area in the center of 1 cm^2, which prevents the electrolyte from reaching the underlying metal. Before all experiments, mild steel samples were thoroughly washed with distilled water, acetone, and ethanol. This was followed by ultrasonic degreasing for 5 minutes using a bath of distilled water and ethanol. The samples were then dried with hot air.

2.2. Preparation of plant extract

Dried leaves of *Portulaca Oleracea* L. were crushed into a fine powder. 5 g was added to 100 ml of 1 M HCl. The mixture was heated and stirred for six hours. The extract was cooled and filtered and then made up to 100 ml with 1 M HCl. This was considered the standard solution. The required concentrations were prepared by diluting the standard solution.

2.3. Preparation of test solution

Analytical grade HCl (35.4%) in distilled water was diluted to create 1 M HCl corrosive media. The utilized extract's concentration ranged from 1 to 4 g·L^{-1}, and the electrolyte volume was 100 ml. To make comparisons and determine the inhibitor efficiency, the 1 M HCl test solution was utilized as a blank.

2.4. Electrochemical cell setup

In this setup, a flat cell offered by Gamry was used. Working electrodes were made from the cut specimens, which had dimensions of 6 cm by 6 cm and a thickness of 0.1 cm. The working electrode's surface area that was exposed to the electrolyte was set to 1 cm^2. The reference electrolyte was a saturated calomel electrode, while the counter electrode made of graphite. The electrolyte in the control experiment was a 1 M HCl solution. Then, as

previously described, the tests were carried out using 1 M HCl and different extract concentrations.

2.5. Potentiodynamic polarization test

In the (PDP) test, a three-electrode cell setup has been used. These electrodes are the working electrode (the metal sample), reference electrode (saturated calomel electrode), and counter electrode (Graphite electrode). 1 M HCl solution was prepared using analytical grade HCl and deionized water to be used as an electrolyte. The temperature was maintained at room temperature (25±2°C). ASTM G5 Standard has been used for making potentiodynamic polarization measurements.

Before the polarization test, the samples were immersed in the electrolyte for 2.5 hours to achieve steady-state conditions. Subsequently, potentiodynamic polarization experiments were initiated by applying a potential to the samples, deviating from the steady state, and measuring the resulting current. The initial point was set at 250 mV below the open circuit potential (OCP). The applied potential was then incrementally increased at a constant sweep rate of 1 mV/sec, concluding the test when the applied potential exceeded the OCP by 250 mV. The experiments were conducted using a reference 600 potentiostat controlled by Gamry framework software version 7.9.1. Additionally, Gamry Echem Analyst software was employed to analyze the polarization curves and extract corrosion parameters such as free corrosion potential (E_{corr}), corrosion current density (i_{corr}), and Tafel anodic and cathodic slopes (β_a, β_c) using the Tafel extrapolation method with a 100 mV interval around the E_{corr} value.

2.6. Weight loss test

Due to its simplicity and availability, researchers have used a weight loss method to measure corrosion rates [26]. First, the samples were cleaned, dried, and weighed using an Ariston digital scale. Then, they were completely immersed in 100 mL of HCl solution without and with different concentrations of POLE at room temperature. After 2 hours of immersion, the sample was removed from the corrosive solution, dehydrated with acetone, ethanol, and distilled water, dried with an air dryer, and weighed again. To test the effect of time, experiments were repeated at immersion periods of 4, 6, 24, and 48 h, with three replicates for each experiment performed. Each sample was weighed three times before and after immersion in the corrosive environment to ensure accurate weight measurement. The average weight is then used to calculate the corrosion rate.

The following equation was utilized to determine weight loss over a specific period:

$$\Delta w = w_0 - w_i \tag{1}$$

where Δw: average weight loss (mg), w_0: average weight loss of the specimen without inhibitors, w_i: average weight loss of the specimen with the inhibitor.

The weight loss data was used to calculate the corrosion rate and inhibition efficiency, using equations 2 and 3 respectively, as outlined in the studies [27, 28].

$$C_{\mathrm{R}}\left(\mathrm{mpy}\right)=\frac{534\cdot\Delta w}{\rho At} \tag{2}$$

where C_R: corrosion rate (mpy), ρ: density of the mild steel (7.78 g/cm^3), A: area of the mild steel sample (cm^2), and t: the period of immersing time.

It is important to note that three replicates were carried out for each test condition (inhibitor concentration and time), and the average corrosion rate values were calculated from these parallel experiments. Using the average of several duplicate samples can help minimize result variability and provide a more precise estimation of the corrosion rate. This contributes to enhancing the dependability of the weight loss test findings and offers a stronger assessment of the inhibitor's effectiveness. The following equation was utilized to determine the percentage of inhibition efficiency %IE:

$$\%IE=\left(\frac{C_{\mathrm{R}_0}-C_{\mathrm{R}}}{C_{\mathrm{R}_0}}\right)\cdot 100\% \tag{3}$$

where C_{R_0} : corrosion rate of the specimens without inhibitor (mpy), and C_{R} : corrosion rate of the specimens with inhibitor (mpy).

2.7. FTIR analysis

Plant extracts are rich in compounds that are responsible for inhibiting corrosion. One of the highly effective and precise methods used to analyze the functional groups present in these extracts is the FTIR. By examining the peaks in the FTIR spectra, valuable information about the functional groups can be obtained. The FTIR spectra in this study were obtained using the Burker ALPHA II infrared spectrometer. A small amount of the 1 M HCl with 4 g/l concentration before and after the weight loss test after 48 h was placed on the sample holder. The FTIR spectra were taken out in the wavelength range of 4000–450 cm^{-1}.

2.8. UV-visible spectroscopy

UV-visible spectroscopy is employed to assess the adsorption characteristics of the inhibitor on a mild steel surface immersed in a 1 M HCl solution, both in the presence and absence of POLE, over a 48-hour immersion period. The UV-visible spectral analysis is conducted using a Shimadzu UV-2250 photometer within a wavelength range spanning 200–800 nm.

3. Results and Discussion

3.1. Potentiodynamic polarization test

Figure 1 shows polarization curves (E) *vs.* ($\log i$) in the Tafel region for mild steel samples in 1 M HCl solution at room temperature. Curves are shown both in the presence and absence of different concentrations of POLE. Table 1 shows the electrochemical parameters, including E_{corr}, i_{corr}, and β_c, β_a, respectively, which were determined by the Tafel curve

extrapolation method [29]. In addition, the percentage inhibition efficiency η (%) and surface coverage (θ) shown in Table 1 were calculated using the equations [30].

$$\eta(\%) = \left(\frac{i^0_{corr} - i_{corr}}{i^0_{corr}} \right) \cdot 100\% \quad (4)$$

$$\theta = \frac{i^0_{corr} - i_{corr}}{i^0_{corr}} \quad (5)$$

where i^0_{corr}: corrosion current density in the absence of POLE in 1 M HCl (μA/cm^2) and i_{corr}: corrosion current density in the presence of POLE in 1 M HCl (μA/cm^2).

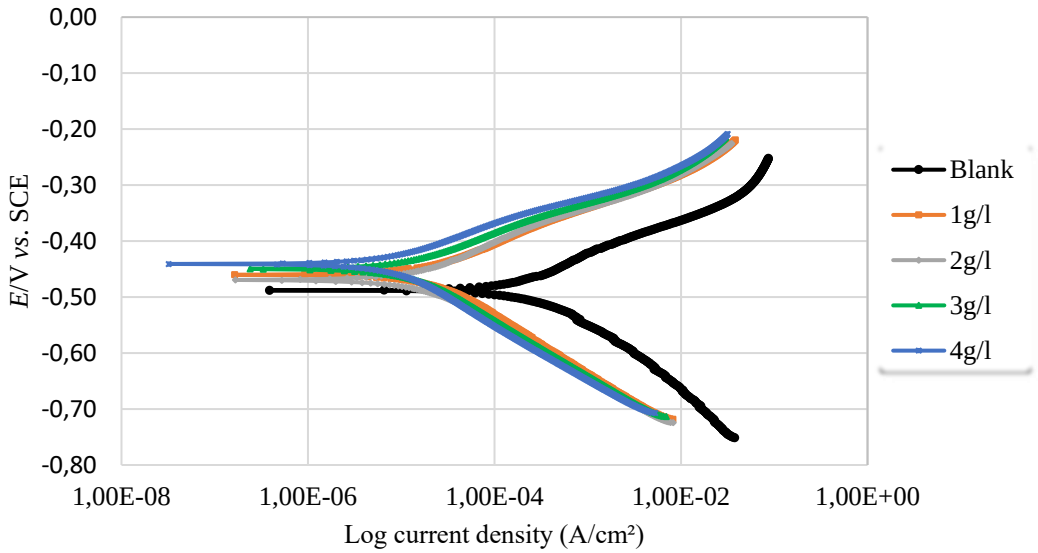

Figure 1. Tafel plots of mild steel in 1 M HCl solution in the absence and presence of different concentrations of POLE.

Table 1. The electrochemical parameters for the mild steel in 1 M HCl solution in the absence and presence of different concentrations of POLE.

C_{inh} (g/L)	β_a (mV/decade)	$-\beta_c$ (mV/decade)	i_{corr} (μA/cm^2)	E_{corr} (mV)	C_R (mpy)	η(%)	θ
Blank	80±16	87±8	112±28	–478±11	67±19	–	
1	84±17	109±12	23±3	–460±10	10±1	80%	0.80
2	84±6	97±4	17±0	–470±5	8±0	85%	0.85
3	71±3	104±1	13±1	–452±0	6±0	88%	0.88
4	72±6	112±8	9±2	–441±5	4±1	92%	0.92

Based on Figure 1, the addition of inhibitors to the corrosive solution resulted in the inhibition of both anodic metal dissolution and cathodic hydrogen evaluation responses. Furthermore, the literature reveals that if the E_{corr} exceeds ±85 mV/SCE compared to the blank acidic solution, the inhibitor is categorized as either cathodic or anodic. Whereas, if the E_{corr} value is less than ±85 mV/SCE the inhibitor is classified as a mixed-type inhibitor [31]. The current study reveals that the POLE serves as a mixed-type corrosion inhibitor as the E_{corr} values are within 85 mV/SCE compared to the blank sample [29]. It is important to note that the introduction of higher concentration levels leads to a significant reduction in both the β_a and β_c. However, the greater variation observed in β_a compared to β_c suggests that the reaction primarily occurs in an anodic manner. The data presented in Table 1 demonstrates that as the inhibitor concentration increases, the corrosion current densities decrease. It is already established that adsorptive inhibitors impede the release of hydrogen gases on the surface of mild steel and/or hinder the dissolution process of mild steel in aggressive solutions by blocking active sites on the surface. Additionally, they can act as a protective barrier, shielding the electrode from the acidic solution [32]. Consequently, it is expected that the inhibition efficiency will increase with a higher concentration of POLE.

3.2. Weight loss test

3.2.1. Effect of concentrations

The weight loss test was conducted at room temperature to study the spontaneous dissolution of mild steel in the presence of POLE as a corrosion inhibitor in 1 M HCl. After immersing the steel for 2 hours, various corrosion parameters were calculated, including C_R and %*IE*, These calculations were done using equations 2, and 3 respectively, and presented graphically in Figures 2 and 3.

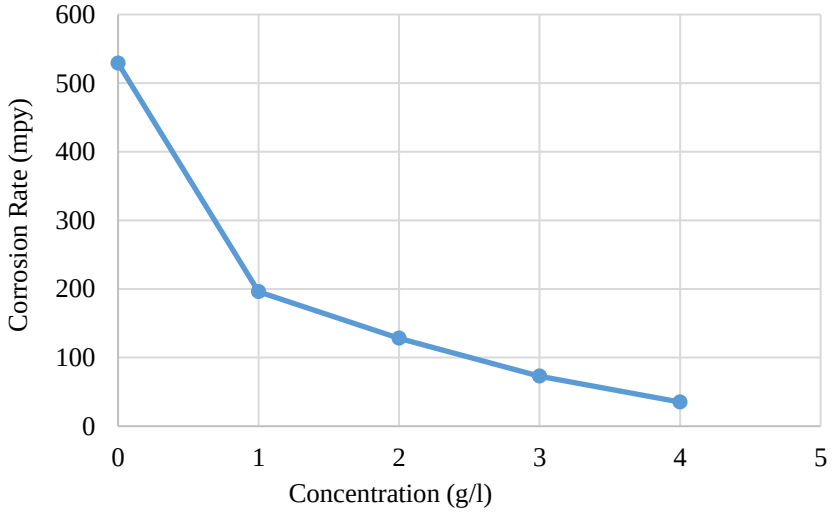

Figure 2. Change of the mild steel corrosion rate as calculated from the weight loss test with different concentrations POLE in 1 M HCl at room temperature.

Figures 2 and 3 demonstrate that the corrosion rate of mild steel decreases as the concentration of POLE increases. Consequently, the inhibition efficiency of POLE also increases with higher concentrations, reaching a value of 93.35% at 4 g/L. This phenomenon can be attributed to the adsorption of POLE molecules on the surface of the mild steel at higher concentrations. This adsorption leads to a greater coverage of the surface and the formation of a thin protective film. This is due to the inhibitor acting as an adsorbent and forming a barrier layer over the metal surface, effectively blocking reaction sites and protecting it from corrosion and dissolution in acidic media. Consequently, the inhibition efficiency increases and the corrosion rate decreases as the number of adsorbed molecules on the mild steel surface increases [6, 33].

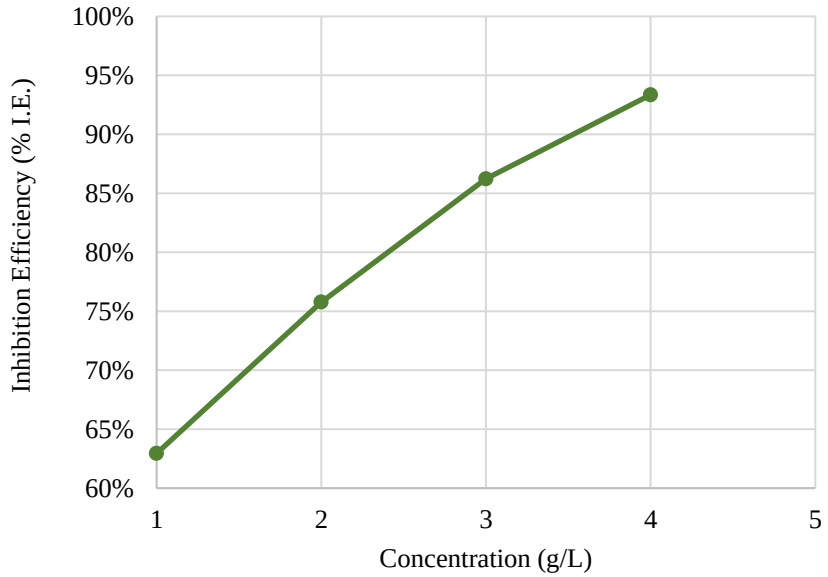

Figure 3. Change of the inhibition efficiency inhibition efficiency (%*IE*) of the mild steel in various concentrations of POLE as calculated from the weight loss test in 1 M HCl at room temperature.

3.2.2. Effect of immersion time

Immersion time is another important parameter for assessing the behavior, inhibition efficiency, and corrosion rate of the inhibitor over a longer immersion period. The inhibition efficiency values (%*IE*) and corrosion rate obtained from the weight loss test at different POLE concentrations in 1 M HCl and at different immersion times of 4, 6, 24, and 48 hours at room temperature are listed in Table 2 and 3 and in Figure 4 shows graphically. Corrosion rate values decrease with immersion time due to the formation of a protective oxide layer on the metal surface. This oxide layer acts as a barrier, protecting the underlying metal from further corrosion. Over time, this passive layer may become thicker and more stable, leading to a decrease in the corrosion rate and increasing the inhibitor efficiency.

Tables 2 and 3 and Figure 4 demonstrate that the maximum inhibition efficiency and minimum corrosion rate were observed after 48 hours of immersion time for all examined

concentrations of POLE. The %*IE* increased and the C_R decreased with increasing immersion time. This phenomenon can be attributed to the fact that sufficient adsorption of the inhibitor molecules on the metal surfaces requires considerable time at relatively low concentrations [34]. The stability and persistence of POLE films on mild steel surfaces in acidic solutions were also indicated, which could last for a long time [35]. Additionally, the %*IE* increased with time due to the formation of inhibitor complexes over the metal surface and the construction of strong bonds with the substrate atoms. As time increased, the production rates of these complexes increased, resulting in higher efficiency and more restrictions on the corrosive electrolyte to reach the metal surfaces [36]. This led to a broader surface cover, blocking the reaction sites and protecting the metal surfaces from corrosion attack and dissolution in acidic media [6]. These findings are consistent with those reported in the literature.

Table 2. Corrosion rate (mpy) values for the mild steel in 1 M HCl solution in the absence and presence of different concentrations of POLE.

Time (h)	Concentration (g/L)				
	Blank	**1 g/L**	**2 g/L**	**3 g/L**	**4 g/L**
	Corrosion rate (mpy)				
2	529±29	196±32	128±6	73±6	35±9
4	526±20	114±25	79±3	54±2	34±6
6	501±17	88±21	62±4	50±4	32±1
24	410±24	62±2	51±2	38±2	25±5
48	361±13	49±1	43±2	33±1	24±1

Table 3. The corrosion inhibition efficiency (%*IE*) values for the mild steel in 1 M HCl solution for different concentrations of POLE after different immersion times.

Time (h)	Concentration (g/L)			
	1 g/L	**2 g/L**	**3 g/L**	**4 g/L**
	Inhibition Efficiency (%IE)			
2	62.95%	75.77%	86.22%	93.35%
4	78.26%	84.95%	88.44%	93.55%
6	82.54%	87.72%	90.06%	93.57%
24	84.94%	87.52%	90.72%	93.84%
48	86.35%	87.98%	90.73%	93.45%

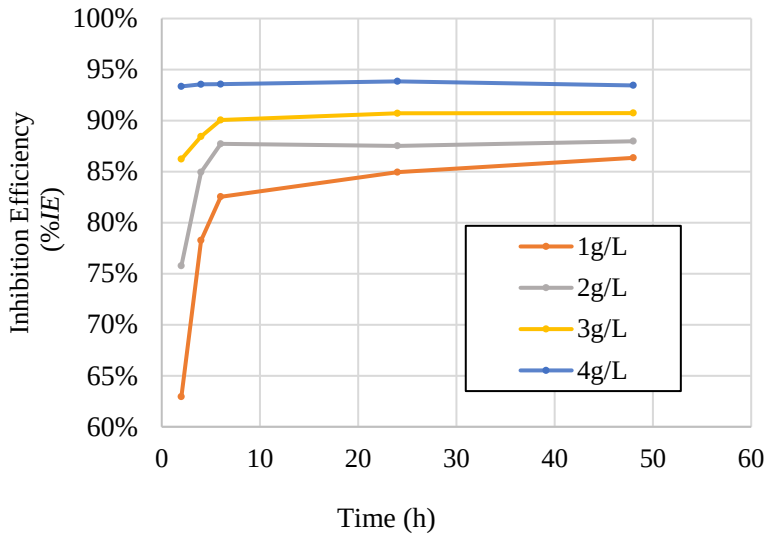

Figure 4. Corrosion inhibition efficiency (%*IE*) for the mild steel in 1 M HCl solution in the absence and presence of different concentrations of POLE after different immersion times.

3.3. Adsorption studies

Adsorption isotherms offer valuable insights into the behavior of adsorption and the nature of interactions between inhibitor molecules and the metal surface. This can be achieved by establishing a relationship between surface coverage and inhibitor concentrations. While numerous isotherm models are mentioned in the literature, the most commonly used ones are Langmuir, Temkin, and Frumkin. The selection of an appropriate isotherm model should be based on a comprehensive analysis of experimental data. One commonly employed technique involves fitting multiple isotherm models to the data and comparing their goodness of fit using statistical measures like the correlation coefficient (R^2). Ultimately, the best isothermal model for a given system is the one that provides the closest fit to the experimental data, accurately describes the underlying adsorption mechanism, and is practical to implement. The efficiency of inhibition is directly proportional to the fraction of adsorbed molecules that cover the surface (θ), where θ=(η/100). The change in C/θ, as a function of the extract concentration, determines the adsorption isotherm that best describes the system. The fit of the obtained data to the Langmuir isotherm can be illustrated by plotting against concentration according to the following equation [30].

$$\text{Langmuir: } \frac{C}{\theta} = \frac{1}{k_{ads}} + c \tag{6}$$

where, C: inhibitor concentrations, θ: the degree of the surface coverage, k_{ads}: the adsorption equilibrium constant.

The linear plots in Figure 5 display (R^2) of 0.9991 for the weight loss test and 0.9992 for the potentiodynamic polarization test, with slopes of 1.040 and 1.0392, respectively.

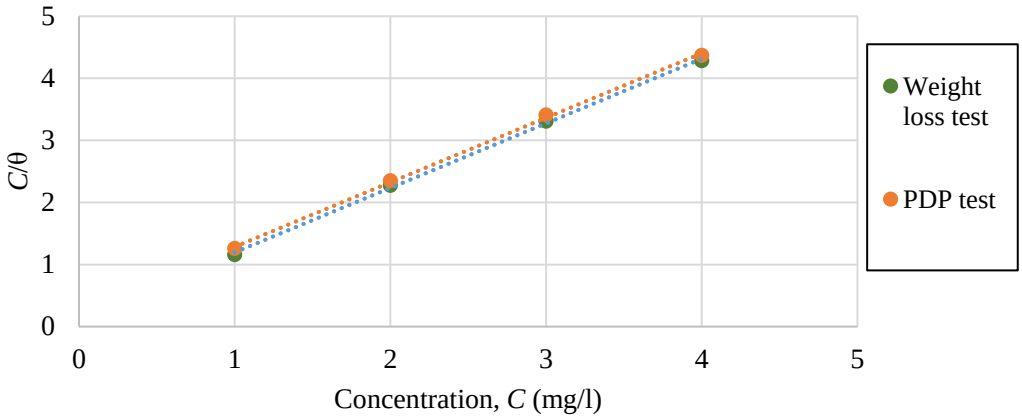

Figure 5. Langmuir isotherm for POLE adsorption on the mild steel surface.

The k_{ads} and R^2 values are listed in Table 5, where R^2 is the degree of fit between the experimental data and the isotherm equation. The plot showed good linearity, with R^2 values close to unity, indicating that the Langmuir model is suitable for describing adsorption. It also indicates strong adsorption of POLE on the surface of mild steel [37]. Langmuir isotherms assume that the adsorption of each molecule on the surface is independent of the other molecules and that the adsorbed surface is homogeneous and has a finite number of adsorption sites [38]. Table 4 includes the k_{ads} and R^2 values, with R^2 indicating the degree of fit between the experimental data and the isotherm equation. The plot displayed strong linearity, with R^2 values near one, indicating that the Langmuir model is appropriate for explaining adsorption. Furthermore, it shows the strong adsorption of POLE on the mild steel surface [37].

Table 4. Langmuir adsorption isotherm parameters for adsorption of POLE on the mild steel surface.

Methods	Intercept	Slope	R^2	k_{ads} (L/g)	ΔG_{ads} (kJ/mol)
Weight loss test	0.1546	1.0400	0.9959	6.4683	–21.74
PDP	0.2462	1.0392	0.9992	4.0617	–20.59

The molecules of the inhibitor gained stability when their free energies were reduced by their adsorption on the surface of the mild steel, where they rearrange themselves or react with the ions or molecules near the surface [39].

The standard adsorption-free energy ΔG^0_{ads} was used to investigate the mechanism of the adsorption of the inhibitors. However, the values ΔG^0_{ads} were calculated according to the following equation (7) to determine the adsorption mechanism:

$$\Delta G^0_{ads} = -RT \ln\left(55.5 k_{ads}\right) \quad (7)$$

The ΔG^0_{ads} value, the adsorption equilibrium constant k_{ads}, R^2, and slopes are shown in Table 4. Overall, negative values of the ΔG^0_{ads} indicate that the adsorption process of the

extracted inhibitor is spontaneous and stable. In addition, according to the literature, the absolute value of the $\Delta G^0_{ads} \leq 20$ kJ/mol is considered to be a physisorption mechanism, which is related to the electrostatic interaction between the positively charged particles of the extracted inhibitor and the negative charge of the metal surface. However, the absolute values of $\Delta G^0_{ads} \geq 40$ kJ/mol were considered as a chemisorption mechanism, which involves the formation of a chemical bond between the extracted inhibitor molecules and the metal surface through electron transfer or sharing. Furthermore, ΔG^0_{ads} values between these ranges are generally attributed to a mixed mechanism, sometimes referred to as physico-chemisorption [40, 41]. The ΔG^0_{ads} values in this work were (–21.74 kJ/mol and –20.59 kJ/mol) for POLE, which shows the adsorption of POLE on the surface of mild steel, which consists of physical adsorption interaction.

3.4. FTIR analysis

POLE showed good anti-corrosion properties due to the presence of antioxidants present in its molecular structure containing heteroatoms such as N, C, and O. For example, POLE contains amino acids and phenols. Infrared plots for 1 M HCl with 4 g/L POLE before and after the weight loss test after 48 hours of immersion are shown in Figure 6. The pre-test FTIR peak and functional group results are shown in Table 5 [42].

Table 5. FTIR peaks value and assigned functional groups for 1 M HCl with 4 g/L POLE before weight loss test.

Wavenumber cm^{-1}	Bond	Functional group
3294.0	O–H stretch	Alcohols
2882.2	S–H stretch	Thiol
2126.8	N=C=N stretch	Carbodiimides
1902.8	C=C=C stretch	Allene
1633.6	N–H bending	Amine
1263.8	C–N stretch	Aromatic amine
610.3	C–Br stretch	Halo-compound

The functional groups have coordinated with Fe^{2+}, forming a Fe^{2+} inhibitor complex that improves the inhibitive influence of the mild steel surface [19]. Moreover, it is well known that OH^{-1} can passive the steel protecting it against corrosion, it reacts with Fe^{2+} ions to form $Fe(OH)_2$ responsible for the steel passivation. Amine is also known to form a good passive film on mild steel surfaces from corrosion, and it can be protonated to give $FeONH^{2+} + H^+$ and probably the $FeONH^{2+}$ complex, which remains on the mild steel surface to protect it [43]. Figure 6 shows shifts and moves in frequencies in the 1 M HCl + 4 g/L POLE spectra after the weight loss test. These results indicate interference between the

POLE and the mild steel surface. The shifts in spectra show an interaction between the POLE and mild steel happened through the mentioned function groups. The missed groups explain the desorption procedure of POLE on the mild steel outer surface [39].

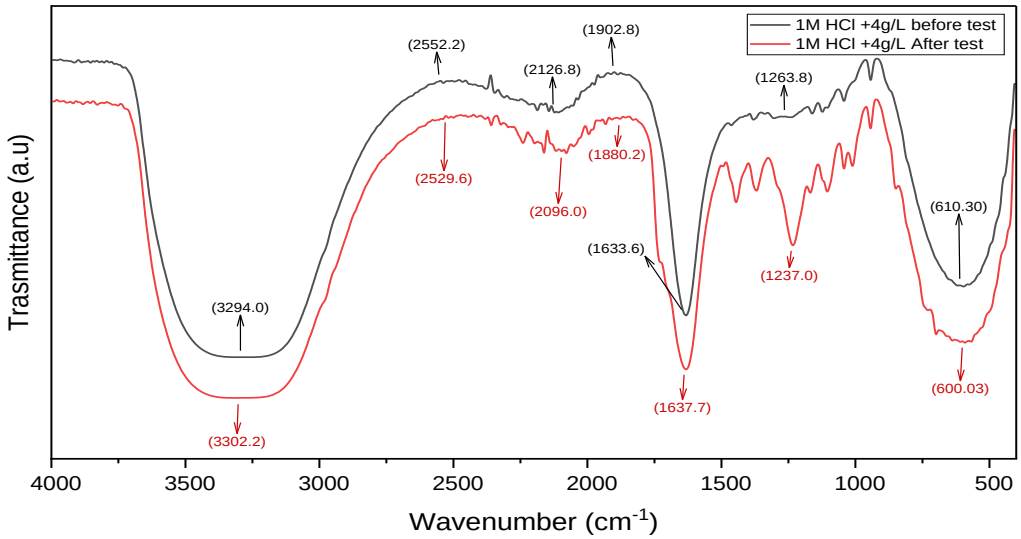

Figure 6. FTIR spectra of 1 M HCl+4 g/L POLE before and after weight loss test.

3.5. UV-visible spectroscopy analysis

UV–visible spectroscopy technique has been used to verify the adsorption phenomenon. UV–visible analysis has been done for the 1 M HCl with 4 g/L of POLE before and after the weight loss test. Figure 7 shows the UV–visible. Spectra of the inhibitor. In the two spectra shown one for UV–visible. Spectra before the corrosion test, and the second one after the corrosion test.

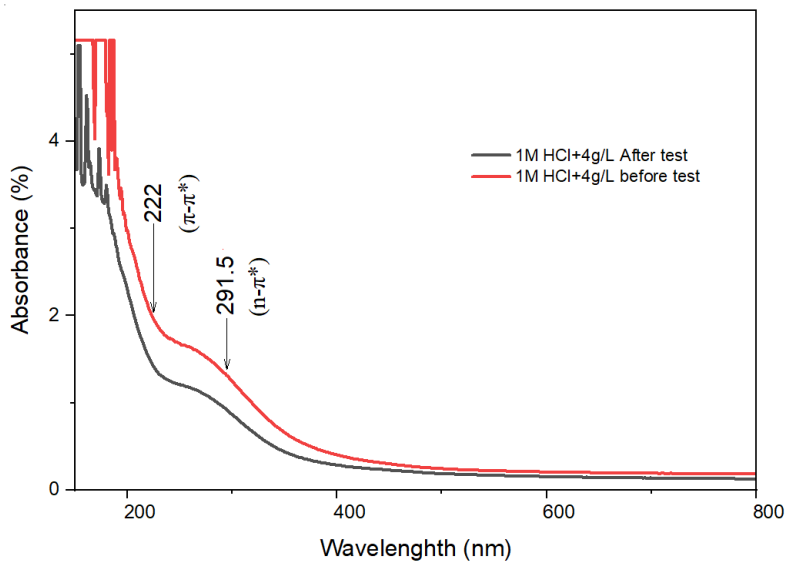

Figure 7. UV–Visible spectra of 1 M HCl+4 g/L Of POLE after and before the weight loss test.

Before the test, the inhibitor shows two adsorption peaks at 222 nm and 291.5 nm. These peaks can be assigned as (π–π*) and (n–π*) transitions. With the help of Figure 7, the graph shows a low adsorption peak after the corrosion test. In comparison between the spectra, there is a significant change in the adsorption band, this can be explained by the inhibitor molecules getting adsorped on the mild steel surface. This result confirms very well with the research in the literature [31, 44].

4. Conclusions

The inhibition performance, as well as the related mechanism of POLE for mild steel protection in 1 M HCl, have been studied, and the following are major conclusions:

1. The results obtained from the corrosion tests demonstrate that POLE acts as an effective inhibitor for mild steel in 1 M HCl.
2. The maximum inhibitory efficiency of 93.84% was observed at a concentration of 4 g/L at room temperature.
3. Potentiodynamic polarization tests suggest that POLE acts as a mixed-type inhibitor, and the anodic impact is predominated.
4. The weight loss test results demonstrate that POLE efficiency increases with concentration and immersion time.
5. The adsorption mechanism for POLE on the mild steel surface follows the Langmuir adsorption isotherm.
6. The ΔG^0_{ads} values indicate that the POLE extract adsorption process is spontaneous and stable, and it is adsorbed on the mild steel surface by physical adsorption.
7. Various functional groups containing heteroatoms and unsaturation in the POLE phytochemical constituents were verified using the FTIR technique.
8. UV-Vis spectroscopy technique verified the formation of coordination bonds between inhibitor molecules and Fe^{2+}.

Funding

This work was supported by a grant from the Deanship of Scientific Research at Jordan University of Science and Technology (JUST) with grant no.166/2019.

References

1. A. Dehghani, G. Bahlakeh and B. Ramezanzadeh, Green *Eucalyptus* leaf extract: A potent source of bio-active corrosion inhibitors for mild steel, *Bioelectrochemistry*, 2019, **130**, 107339. doi: 10.1016/j.bioelechem.2019.107339
2. A. Sedik, D. Lerari, A. Salci, S. Athmani, K. Bachari, İ.H. Gecibesler and R. Solmaz, Dardagan Fruit extract as eco-friendly corrosion inhibitor for mild steel in 1 M HCl: Electrochemical and surface morphological studies, *J. Taiwan Inst. Chem. Eng.*, 2020, **107**, 189–200. doi: 10.1016/j.jtice.2019.12.006

3. L.O. Olasunkanmi and E.E. Ebenso, Experimental and computational studies on propanone derivatives of quinoxalin-6-yl-4,5-dihydropyrazole as inhibitors of mild steel corrosion in hydrochloric acid, *J. Colloid Interface Sci*., 2020, **561**, 104–116. doi: 10.1016/j.jcis.2019.11.097
4. D. Senthil, R. Saratha and R. Vasantha, Corrosion inhibition of mild steel in hydrochloric acid medium using plant extracts, *Int. J. Sci*., 2016, **5**, no. 12, 3324–3340.
5. M. El Faydy, M. Rbaa, L. Lakhrissi, B. Lakhrissi, I. Warad, A. Zarrouk and I.B. Obot, Corrosion protection of carbon steel by two newly synthesized benzimidazol-2-ones substituted 8-hydroxyquinoline derivatives in 1 M HCl: Experimental and theoretical study, *Surf. Interfaces*., 2019, **14**, 222–237. doi: 10.1016/j.surfin.2019.01.005
6. M. Mobin, M. Basik and J. Aslam, Pineapple stem extract (bromelain) as an environmentally friendly novel corrosion inhibitor for low carbon steel in 1 M HCl, *Measurement*, 2019, **134**, 595–605. doi: 10.1016/j.measurement.2018.11.003
7. S.A. Umoren, M.M. Solomon, I.B. Obot and R.K. Suleiman, A critical review on the recent studies on plant biomaterials as corrosion inhibitors for industrial metals, *J. Ind. Eng. Chem*., 2019, **76**, 91–115. doi: 10.1016/j.jiec.2019.03.057
8. C. Verma, E.E. Ebenso, I. Bahadur and M.A. Quraishi, An overview on plant extracts as environmental sustainable and green corrosion inhibitors for metals and alloys in aggressive corrosive media, *J. Mol. Liq*., 2018, **266**, 577–590. doi: 10.1016/j.molliq.2018.06.110
9. Z. Sanaei, M. Ramezanzadeh, G. Bahlakeh and B. Ramezanzadeh, Use of *Rosa canina* fruit extract as a green corrosion inhibitor for mild steel in 1 M HCl solution: A complementary experimental, molecular dynamics and quantum mechanics investigation, *J. Ind. Eng. Chem*., 2019, **69**, 18–31. doi: 10.1016/j.jiec.2018.09.013
10. A. El Yaktini, A. Lachiri, M. El Faydy, F. Benhiba, H. Zarrok, M. El Azzouzi, M. Zertoubi, M. Azzi, B. Lakhrissi and A. Zarrouk, Practical and theoretical study on the inhibitory influences of new azomethine derivatives containing 8-hydroxyquinoline moiety for the corrosion of carbon steel in 1 M HCl, *Orient. J. Chem*., 2018, **34**, no. 6, 3016–3029. doi: 10.13005/ojc/340643
11. N. El Aouni, R. Hsissou, Z. Safi, S. Abbout, F. Benhiba, J. El Azzaoui, R. Haldhar, N. Wazzan, L. Guo, H. Erramli, A. Elharfi, A. El Bachiri and M. Rafik, Performance of two new epoxy resins as potential corrosion inhibitors for carbon steel in 1 M HCl medium: Combining experimental and computational approaches, *Colloids Surf., A*., 2021, **626**, 127066. doi: 10.1016/j.colsurfa.2021.127066
12. A. Thoume, A. Elmakssoudi, D.B. Left, N. Benzbiria, F. Benhiba, M. Dakir, M. Zahouily, A. Zarrouk, M. Azzi and M. Zertoubi, Amino acid structure analog as a corrosion inhibitor of carbon steel in 0.5 M H_2SO_4: Electrochemical, synergistic effect and theoretical studies, *Chem. Data Collect*., 2020, **30**, 100586. doi: 10.1016/j.cdc.2020.100586

13. N. Rajae, B. Fouad, R. Youssef, O. Moussa, C. Mohammed, O. Hassan, W. Ismail and Z. Abdelkade, Corrosion Inhibition Study of 5,5-diphenylimidazolidine-2,4-dione for Mild Steel Corrosion in 1 M HCl Solution: Experimental, Theoretical Computational and Monte Carlo Simulations Studies, *Anal. Bioanal. Electrochem*., 2018, **10**, 1375–1398.
14. H. Elmsellem, Y. El Ouadi, M. Mokhtari, H. Bendaif, H. Steli, A. Aouniti, A.M. Almehdi, I. Abdel-Rahman, H.S. Kusuma and B. Hammouti, A natural antioxidant and an environmentally friendly inhibitor of mild steel corrosion: A commercial oil of basil (*Ocimum basilicum L.*), *J. Chem. Technol. Metall.*, 2019, **54**, no. 4, 742–749.
15. M. Jokar, T.S. Farahani and B. Ramezanzadeh, Electrochemical and surface characterizations of morus alba pendula leaves extract (MAPLE) as a green corrosion inhibitor for steel in 1 M HCl, *J. Taiwan Inst. Chem. Eng*., 2016, **63**, 436–452. doi: 10.1016/j.jtice.2016.02.027
16. G. Khan, W.J. Basirun, H. Binti, M. Ali, L. Faraj and G.M. Khan, Application of Natural Product Extracts as Green Corrosion Inhibitors for Metals and Alloys in Acid Pickling Processes-A review, *Int. J. Electrochem. Sci*., 2015, **10**, no. 8, 6120–6134.
17. M.T. Hayajneh, M.A. Almomani and W.M. Alsharman, A study on Jordanian green natural agro wastes as potential inhibitors of mild steel corrosion in hydrochloric acid solution, *Green Mater*., 2023, **40**, 1–14. doi: 10.1680/jgrma.21.00040
18. M.A. Almomani, M.T. Hayajneh and W.M. Alsharman, *Ceratonia siliqua* pulp extracts as a green corrosion inhibitor for mild carbon steel in 1 M HCl, *Int. J. Corros. Scale Inhib*., 2023, **12**, no. 2, 793–810. doi: 10.17675/2305-6894-2023-12-2-23
19. A. Dehghani and B. Ramezanzadeh, *Rosemary* extract inhibitive behavior against mild steel corrosion in tempered 1 M HCl media, *Ind. Crops Prod*., 2023, **193**, 116183. doi: 10.1016/j.indcrop.2022.116183
20. M.R. Rathod, S.K. Rajappa and A.A. Kittur, Garcinia livingstonei leaves extract influenced as a mild steel efficient green corrosion inhibitor in 1 M HCl solution, *Mater. Today: Proc*., 2021, **54**, 786–796. doi: 10.1016/j.matpr.2021.11.084
21. A.M. Guruprasad and H.P. Sachin, Novel cost-effective aqueous *Amorphophallus paeoniifolius* leaves extract as a green corrosion inhibitor for mild steel corrosion in hydrochloric acid medium: A detailed experimental and surface characterization studies, *Chem. Data Collect*., 2021, **34**, 100734. doi: 10.1016/j.cdc.2021.100734
22. M. Keramatinia, B. Ramezanzadeh and M. Mahdavian, Green production of bioactive components from herbal origins through one-pot oxidation/polymerization reactions and application as a corrosion inhibitor for mild steel in HCl solution, *J. Taiwan Inst. Chem. Eng*., 2019, **105**, 134–149. doi: 10.1016/j.jtice.2019.10.005
23. U.R. Palaniswamy, B.B. Bible and R.J. Mcavoy, Effect of Nitrate: Ammonium Nitrogen Ratio on Oxalate Levels of Purslane, *Trends in New Crops and New Uses*, 2002, 453–455.

24. X. Xu, L. Yu and G. Chen, Determination of flavonoids in *Portulaca oleracea* L. by capillary electrophoresis with electrochemical detection, *J. Pharm. Biomed. Anal*., 2006, **41**, no. 2, 493–499. doi: 10.1016/j.jpba.2006.01.013
25. U.R. Palaniswamy, R.J. McAvoy and B.B. Bible, Stage of harvest and polyunsaturated essential fatty acid concentrations in purslane (*Portulaca oleracea*) leaves, *J. Agric. Food Chem*., 2001, **49**, no. 7, 3490–3493. doi: 10.1021/jf0102113
26. E.B. Agbaffa, E.O. Akintemi, E.A. Uduak and O.E. Oyeneyin, Corrosion inhibition potential of the methanolic crude extract of Mimosa pudica leaves for mild steel in 1 M hydrochloric acid solution by weight loss method, *Sci. Lett*., 2021, **15**, no. 1, 23. doi: 10.24191/sl.v15i1.11791
27. M.H. Sliem, M. Afifi, A.B. Radwan, E.M. Fayyad, M.F. Shibl, F.E.T. Heakal and A.M. Abdullah, AEO7 Surfactant as an Eco-Friendly Corrosion Inhibitor for Carbon Steel in HCl solution, *Sci. Rep*., 2019, **9**, 1–16. doi: 10.1038/s41598-018-37254-7
28. P. Muthukrishnan, P. Prakash, B. Jeyaprabha and K. Shankar, Stigmasterol extracted from *Ficus hispida* leaves as a green inhibitor for the mild steel corrosion in 1 M HCl solution, *Arabian J. Chem*., 2019, **12**, no. 8, 3345–3356. doi: 10.1016/j.arabjc.2015.09.005
29. G. Fekkar, F. Yousfi, H. Elmsellem, M. Aiboudi, M. Ramdani, Abdel-Rahman, B. Hammouti and L. Bouyazza, Eco-friendly *chamaerops humilis* l. Fruit extract corrosion inhibitor for mild steel in 1 M HCl, *Int. J. Corros. Scale. Inhib*., 2020, **9**, no. 2, 446–459. doi: 10.17675/2305-6894-2020-9-2-4
30. W. Zhang, H.J. Li, M. Wang, L.J. Wang, A.H. Zhang and Y.C. Wu, Highly effective inhibition of mild steel corrosion in HCl solution by using pyrido[1,2-a]benzimidazoles, *New J. Chem*., 2019, **43**, no. 1, 413–426. doi: 10.1039/C8NJ04028A
31. R. Haldhar and D. Prasad, Corrosion Resistance and Surface Protective Performance of Waste Material of *Eucalyptus globulus* for Low Carbon Steel, *J. Bio Tribo Corros*., 2020, **6**, no. 48, 1–13. doi: 10.1007/s40735-020-00340-3
32. M. Khattabi, F. Benhiba, S. Tabti, A. Djedouani, A. ElAssyry, R. Touzani, I. Warad, H. Odda and A. Zarrouk, Performance and computational studies of two soluble pyran derivatives as corrosion inhibitors for mild steel in HCl, *J. Mol. Struct*., 2019, **1196**, 231–244. doi: 10.1016/J.MOLSTRUC.2019.06.070
33. J. Bhawsar, P.K. Jain and P. Jain, Experimental and computational studies of *Nicotiana tabacum* leaves extract as green corrosion inhibitor for mild steel in acidic medium, *Alexandria Eng. J*., 2015, **54**, no. 3, 769–775. doi: 10.1016/j.aej.2015.03.022
34. O.A. Akinbulumo, O.J. Odejobi and E.L. Odekanle, Thermodynamics and adsorption study of the corrosion inhibition of mild steel by *Euphorbia heterophylla* L. extract in 1.5 M HCl, *Results Mater*., 2020, **5**. doi: 10.1016/j.rinma.2020.100074
35. R. Karthikaiselvi, S. Subhashini and R. Rajalakshmi, Poly (vinyl alcohol – aniline) water-soluble composite as corrosion inhibitor for mild steel in 1 M HCl, *Arabian J. Chem*., 2012, **5**, no. 4, 517–522. doi: 10.1016/j.arabjc.2010.09.020

36. M.T. Majd, S. Asaldoust, G. Bahlakeh, B. Ramezanzadeh and M. Ramezanzadeh, Green method of carbon steel effective corrosion mitigation in 1 M HCl medium protected by Primula vulgaris flower aqueous extract via experimental, atomic-level MC/MD Simulation and Electronic-level DFT Theoretical Elucidation, *J. Mol. Liq*., 2019, **284**, 658–674. doi: 10.1016/j.molliq.2019.04.037
37. R.S. Nathiya, S. Perumal, V. Murugesan and V. Raj, Evaluation of extracts of *Borassus flabellifer* dust as green inhibitors for aluminium corrosion in acidic media, *Mater. Sci. Semicond. Process*., 2019, **104**, 104674. doi: 10.1016/j.mssp.2019.104674
38. H. Hassannejad and A. Nouri, Sunflower seed hull extract as a novel green corrosion inhibitor for mild steel in HCl Solution, *J. Mol. Liq*., 2018, **254**, 377–382. doi: 10.1016/j.molliq.2018.01.142
39. A.E.A.S. Fouda, S.M. Rashwan, M.M. Kamel and E.A. Haleem, Juglans regia extract (JRE) as eco-friendly inhibitor for aluminum metal in hydrochloric acid medium, Biointerface Res. Appl. Chem., 2020, **10**, no. 5, 6398–6416. doi: 10.33263/BRIAC105.63986416
40. E. Ituen, O. Akaranta, A. James and S. Sun, Green and sustainable local biomaterials for oilfield chemicals: *Griffonia simplicifolia* extract as a steel corrosion inhibitor in hydrochloric acid, *Sustainable Mater. Technol*., 2017, **11**, 12–18. doi: 10.1016/j.susmat.2016.12.001
41. Q. Wang, B. Tan, H. Bao, Y. Xie, Y. Mou, P. Li, D. Chen, Y. Shi, X. Li and W. Yang, Evaluation of *ficus tikoua* leaves extract as an eco-friendly corrosion inhibitor for carbon steel in HCl Media, *Bioelectrochemistry*, 2019, **128**, 49–55. doi: 10.1016/j.bioelechem.2019.03.001
42. S.D. Shetty, P. Shetty and H.V.S. Nayak, The inhibition action of *N*-furfuryl-*N*'-phenyl thiourea on the corrosion of mild steel in acid media, *J. Serb. Chem. Soc*., 2006, **71**, no. 10, 1073–1082, doi: 10.2298/JSC0610073S
43. M.J. Garcia-Ramirez, G.F. Dominguez Patiño, J.G. Gonzalez-Rodriguez, M.L. Dominguez-Patiño and J.A. Dominguez-Patiño, A Study of *Eruca vesicaria*, *Bromelia hemisphaerica* and *Erythrina americana* as Green Corrosion Inhibitors for Carbon Steel in Sulfuric Acid, *Adv. Mater. Phys. Chem*., 2016, **6**, no. 2, 9–20. doi: 10.4236/ampc.2016.62002
44. A. Saxena, D. Prasad, R. Haldhar, G. Singh and A. Kumar, Use of *Saraca ashoka* extract as green corrosion inhibitor for mild steel in 0.5 M H_2SO_4, *J. Mol. Liq*., 2018, **258**, 89–97. doi: 10.1016/j.molliq.2018.02.104

♦♦♦